Chapter 2

Theoretical Background

2.1 The Standard Model

The Standard Model is a theory that describes properties and interactions of all particles known to date, except the case of neutrino oscillations. The model is widely accepted because it has been tested to a high level of precision. It can also provide accurate predictions to many phenomena in high energy physics experiments. It is an essential part for experimentalists in the field to understand the theory and be able to apply it to explain their experimental results.

In the Standard Model, elementary particles are classified in three categories: leptons, quarks and mediators. The leptons and quarks are half-integer-spin particles or *fermions*, while the force mediators are whole-integer-spin particles or *bosons*. The leptons and quarks are grouped into three generations as shown in Table 2.1 - Table 2.3 The values of mass of leptons and quarks are from Ref. [2].

Table 2.1: First Generation Fermions

Type	Particle	Symbol	Spin	Charge	Mass (MeV/c^2)
Leptons	Electron Neutrino	ν_e	$\frac{1}{2}$	0	$< 3 \times 10^{-6}$
	Electron	e	$\frac{1}{2}$	-1	0.51
Quarks	Up Quark	u	$\frac{1}{2}$	$\frac{2}{3}$	$\sim 1.5 - 4$
	Down Quark	d	$\frac{1}{2}$	$-\frac{1}{3}$	$\sim 4 - 8$

Table 2.2: Second Generation Fermions

Type	Particle	Symbol	Spin	Charge	Mass (MeV/c^2)
Leptons	Muon Neutrino	ν_μ	$\frac{1}{2}$	0	< 0.19
	Muon	μ	$\frac{1}{2}$	-1	105.66
Quarks	Charm Quark	c	$\frac{1}{2}$	$\frac{2}{3}$	$\sim 1.15 - 1.35$
	Strange Quark	s	$\frac{1}{2}$	$-\frac{1}{3}$	$\sim 80 - 130$

Table 2.3: Third Generation Fermions

Tyep	Particle	Symbol	Spin	Charge	Mass (MeV/c^2)
Leptons	Tau Neutrino	ν_τ	$\frac{1}{2}$	0	< 18.2
	Tau	τ	$\frac{1}{2}$	-1	1776.99
Quarks	Top Quark	t	$\frac{1}{2}$	$\frac{2}{3}$	174.3
	Bottom Quark	b	$\frac{1}{2}$	$-\frac{1}{3}$	$\sim 4.1 - 4.4$

The first generation fermions are constituent particles of ordinary matter. The second and third generations are unstable elementary particles, which can only be seen in high-energy processes. All neutrinos in the Standard Model are assumed to be massless. However, recent discoveries of neutrino from solar and atmospheric experiments have shown some hints that neutrinos do have masses. This is the sole evidence of deviation from the Standard Model.

The interaction of the leptons and quarks is made possible by the exchange of the mediator particles or bosons. The mediator particles can also be called "gauge boson" to give a mathematical sense. The commonly known gauge boson is photon, a mediator of electromagnetic force. For the weak forces, its mediators are three gauge bosons, W^-, W^+ and Z^0 and for the strong force, its mediator is the zero-mass gluon. Properties of all gauge bosons are listed in Table 2.4 The values of mass of the gauge bosons are from Ref. [2].

Table 2.4: Gauge Bosons

Particle	Symbol	Spin	Charge	Mass (GeV/c^2)
Photon	γ	1	0	0
W Boson	$W^{\pm}$	1	±1	80.425 ± 0.038
Z Boson	Z^0	1	0	91.1876 ± 0.0021
Gluon	g	1	0	0
Graviton	G	2	0	0

2.2 Proton Substructure

The knowledge of the substructure of proton is of fundamentally essential for understanding the works carried out within the proton-proton collider. In order to determine the interaction rates and cross-section of processes occurring from collision of bunches of protons, we need to understand the components inside the protons and how they interact.

Since the discovery of the nucleus by Sir Ernest Rutherford in 1912 and the neutron by James Chadwick in 1932, neutrons and protons were believed to be point-like particles like electrons or photons for almost half a century, until 1969, while Hofsteadter was trying to measure the charge distribution of neutron. He accidentally discovered that the neutron particles were made of some smaller parts. Not long after Hofsteadter's discovery, a number of electron-proton scattering experiments carried out at SLAC in later years had unveiled that protons also contain substructure, which were later named *partons*.

The experiment carried out at SLAC could be perceived as an advanced version of Rutherford's experiment, with the nucleons acting as the gold atoms and the partons acting as the atoms' core constituents. These constituents of the nucleon, or namely parton, were hinted as *quarks*, which were previously proposed by Murray Gell-Mann in 1964. In his work [3], Gell-Mann suggested that quarks were basic constituent of all hadrons and of which he nicely arranged them in a beautiful geometrical patterns under an *SU(3)* group symmetry principle.

However, this suggestion appeared to be merely a mathematical and theoretical consideration. Until late 1960s, Bjorken [4], [5] and Feynman [6] proposed the new theoretical model of proton substructure, *the parton model*, that nicely described the results obtained from deep inelastic scattering experiments of electrons from protons.

In their proposal, Bjorken [4], [5] and Feynman [6] hypothesized that inside the proton was a collection of a small number of objects, *partons*, which were loosely bounded together. These objects consist of quarks (and its anti-particles), which are fermions with electric charge and some neutral elements responsible for binding these objects together, which now known as gluons.

The hypothesis suggested by Bjorken and Feynman was later confirmed in 1974 under a newly developed Quantum Chromodynamics (QCD). More specifically, the hypothesis of loosely interacting partons is one of essential ingredients in the asymptotic freedom and hadronization by colour confinement. Recently, for the discovery of the asymptotic freedom, David J. Gross, H. David Politzer and Frank Wilczek were awarded the 2004 Physics Nobel Prize.

2.3 The Parton Distribution Function

In current QCD theory, the parton inside the proton composed of three portions: valence quarks, gluons and sea quarks. Valence quarks inside the proton are two up-quarks and one down-quark. Gluons are strong force mediator which are exchanged among quarks to form an interaction that holds them together. The sea quarks are grouped as short-lived quarks-antiquarks pairs and their associated gluons. Even though they do not live very long, sea quarks play an important role in proton-proton collision physics.

So far, there is no definite theoretical model that can accurately describes how quarks and gluons reside inside the proton. The best model which give the most accurate results relies on the *Parton Distirbution Function* or shortly PDF.

PDF are continually being corrected and produced by groups of theoretical physicists. New sets of PDF keep replacing the previous ones. While the old sets are PDF calculated to the leading order (LO) of the Altarelli-Parisi equations [7], the new sets are the ones corrected to the next-to-leading order (NLO) and the next-to-next-to-leading order (NNLO).

The three main groups regarded as major developers of new sets of PDF are GRV, CTEQ and MRST groups. The names of the authors of each group are displayed in Table 2.5 below.

Table 2.5: Groups of PDF developers

Group	Authors
GRV group	M. Glück, E. Reya and A. Vogt
CTEQ group	J. Huston, J. G. Morfin, J. Owens, J. Qui, et al
MRST group	A. D. Martin, R. G. Roberts, W. J. Stirling and R. S. Thorne

With better PDF sets, we can simulate particle interactions and obtain physical quantities as close to the ones from the real experiment as possible. In this work, we have used the currently available PDF sets, CTEQ5L, for our event generator. This PDF set is developed by CTEQ group [8] and corrected to Leading Order (LO).

2.4 The Weak Interaction and $W^{\pm}$ and Z^0 Particles

In the Standard Model, the weak interaction among quarks and leptons is created by an exchane of weak force carriers or mediators, the $W^{\pm}$ and Z^0 bosons. Weak interaction is presented among all kinds of quarks and leptons; but most of the time it is dominated by much more powerful electromagnetic or strong interaction. The weak interactions are categorized into three types, based on either the initial particles that produce the interaction or the type of particles in the final states. When only leptons involve in either the initial state or final state, the process is called *leptonic interaction or leptonic decay*. Similarly, when only hadrons take part in the weak interaction, the interaction is named *non-leptonic*. For the case that both leptons and hadrons play the role in creating weak interaction, the process is called *semi-leptonic*..

One distinct feature that distinguishes weak interaction from strong and electromagnetic interaction is its ability to change *quarks flavor*. To determine whether an interaction is weak, not strong or electromagnetic, is to see whether the quarks flavor has been changed in the process. If it does, for example, from u quark to d quark, then that interaction is weak interaction.

The $W^{\pm}$ and Z^0 had been long predicted to exist in the electroweak theory by three physics Nobel laureates, Sheldon Glashow, Steven Weinberg and Abdus Salam. They were first observed in 1983 through a UA1 and UA2 detector of Super Proton-AntiProton Synchroton ($Sp\bar{p}S$) at CERN [9], [10] via the following decay modes:

$$u + \bar{d} \rightarrow W^+ \rightarrow e^+ + \nu_e, \mu^+ + \nu_\mu, \tag{2.1}$$

$$\bar{u} + d \rightarrow W^- \rightarrow e^- + \bar{\nu_e}, \mu^- + \bar{\nu_\mu}, \tag{2.2}$$

$$u + \bar{u} \rightarrow Z^0 \rightarrow e^+e^-, \mu^+\mu^- and \tag{2.3}$$

$$d + \bar{d} \rightarrow Z^0 \rightarrow e^+e^-, \mu^+\mu^- \tag{2.4}$$

In the first line of decay mode in Eq. (2.1), the cross -section of W^+ production at rest in the center-of-mass frame can be found by using the *Breit-Wigner resonance formula* [11]:

$$\sigma(u\bar{d} \rightarrow W^+ \rightarrow e^+\nu_e) = \frac{1}{N_c}\frac{4\pi\lambda^2\Gamma_{u\bar{d}}\Gamma_{e\nu}/4}{(2s_d+1)(2s_u+1)[(E-M_W)^2+\Gamma^2/4]}\frac{2J+1}{3} \tag{2.5}$$

where $s_d = s_u = \frac{1}{2}$ are the spin of the quarks, M_W is the mass of W$^{\pm}$ boson, J is the angular momentum of the quarks, E is an invariant mass of $u\bar{d}$, $\lambda = 2/E$ is the de Broglie center-of-mass wavelength of the colliding particles in units setting $h = c = 1$ and $\Gamma, \Gamma_{u\bar{d}}, \Gamma_{e\nu}$ are total and partial widths for the decay. In case of the Z^0 production, the cross-section is about 10 times smaller than that of $W^\pm$ because it has to take account the weak mixing parameter $\sin^2\theta_W$ [12].

By integrating the cross-section of quarks in Eq. (2.5) over the $W^\pm$'s and Z^0's width and the quarks' momentum distribution inside the nucleon, we obtain the cross-sections for the reactions $q\bar{q} \to Z^0 \to e^+e^-$ and $q\bar{q} \to W^\pm \to e^+\nu$.

In the case of the $Sp\bar{p}S$ collider, which produced 270 GeV protons and 270 GeV antiprotons, the cross -section for $q\bar{q} \to Z^0 \to e^+e^-$ is on the order of 0.1 nb (1 nb $\equiv 10^{-33}$ cm^2) and for $q\bar{q} \to W^\pm \to e^\pm\nu(\bar{\nu})$ the cross-section is on the order of 1 nb. Comparing to the size of 40 mb total cross-section for the $p\bar{p}$ collision, the $W^\pm$'s and Z^0 production are extremely rare, about 10 millions smaller. In Fig. 2.1, some prediction cross-sections of the $W^\pm$ and Z^0 production are given as function of center of mass energy.

Besides the mass of $W^\pm$ and Z^0 given in the first section of this chapter, we provide some important quantities of the three bosons in Table 2.6 and Table 2.7 in this subsection. (The numbers are from Ref. [2].)

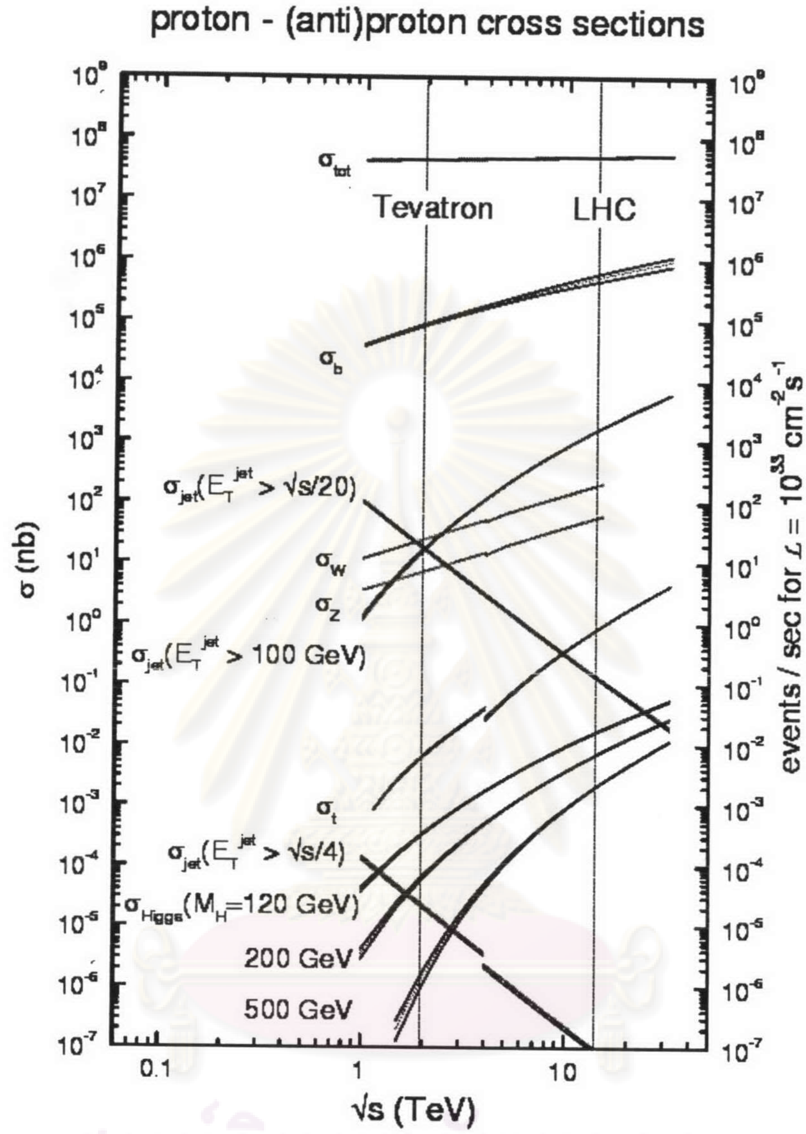

Figure 2.1: Expected cross-sections as a function of energy in the center of mass system for protón-proton collision. (picture excerpted from G. Fluüge. Future Research in High Energy Physics. In N. Ellis and M. B. Gavela, editors, *1993 European School of High Energy Physics*, Yellow reports. (1994): CERN 94-04.)

Table 2.6: The decay modes of $W^{\pm}$ bosons

$W^{\pm}$			
Decay modes	Fraction (Γ_i/Γ)	Full width	Mean life
$e^{+}\nu$	$(10.72 \pm 0.16)\%$	$\Gamma = 2.124 \pm 0.041$ GeV	$\simeq 3 \times 10^{-25}$ s
$\mu^{+}\nu$	(10.57 ± 0.22) %		
$\tau^{+}\nu$	(10.74 ± 0.27) %		

Table 2.7: The decay modes of Z^0 bosons

Z^0			
Decay modes	Fraction (Γ_i/Γ)	Full width	Mean life
$e^{+}e^{-}$	(3.363 ± 0.004) %	$\Gamma = 2.4952 \pm 0.0023$ GeV	$\simeq 2.6 \times 10^{-25}$ s
$\mu^{+}\mu^{-}$	(3.366 ± 0.007) %		
$\tau^{+}\tau^{-}$	(3.370 ± 0.008) %		

2.5 The Luminosity

In year 2007, the LHC will begin generating proton-proton collisions with total center-of-mass energy of 14 TeV and a goal luminosity $\mathcal{L} = 10^{34}$ cm^{-2}s^{-1}. All detectors built to support various experiment programs of the LHC are expected to deliver high statistical data, whose precision of measurement will be restricted by systematic effects and, in several conditions, by the uncertainty in the measurement of the luminosity $\mathcal{L}$. For example, precision measurements in the Higgs sector of typical accuracy of about 7%, for a wide range of possible Higgs mass, require the uncertainty in the luminosity to be $\leq 5\%$. According to the CMS technical proposal, the CMS experiment programs **"will aim to measure the [proton-proton] luminosity at CMS with a precision of better than 5% This precision is chosen to match approximately the precision which theorists expect to achieve in predictions for hard scattering cross-sections at LHC energies at the time CMS takes data."**.

There are three types of luminosity for a colliding beam machine: an *absolute luminosity*, an average luminosity measured from each run, required for determining experimental cross-sections of observed physical processes; a *relative luminosity*, measured for duration of each run, required for determining the partial luminosity for each run; an *instantaneous relative luminosity* required to indicate for the beam quality. The instantaneous luminosity is also required in the data analysis such as for correcting pile-up effects.

In this thesis, the *relative luminosity* will be called shortly as *"luminosity"* since it is the only kind of luminosity that will be discussed.

The luminosity of any given events is related to the cross-section of that event and the event rate by

$$R_{evt} = \sigma \cdot \mathcal{L} \tag{2.6}$$

where R_{evt} is the event rate, σ is the cross-section of a given process and $\mathcal{L}$ is the luminosity. While the event rate R_{evt} can only be obtained from experiment, the cross-section σ can be obtained from either experiment or theoretical calculation.

Beside measuring the luminosity using Eq. (5.3), the luminosity can also be obtained from beam parameters by:

$$\mathcal{L} = f\frac{n_1 n_2}{4\pi\rho_x\rho_y} \tag{2.7}$$

where n_1 and n_2 are the number of protons in each colliding bunches, f is revolution frequency and ρ_x and ρ_y characterize the Gaussian transverse beam profiles in the horizontal and vertical directions respectively. More technically, we can express Eq. (2.7) in terms of the two more practical beam parameters, i.e. *the transverse emittance*, ϵ and *amplitude function*, β, at interaction point denoted by, β^*:

$$\mathcal{L} = f\frac{n_1 n_2}{4\sqrt{\epsilon_x \beta_x^* \epsilon_y \beta_y^*}}. \tag{2.8}$$

The transverse emittance, ϵ, is a beam quality reflecting the process of bunch preparation, extending all the way back to the source of hadrons and, in the case of electrons, mostly dependent on synchrotron radiation. The amplitude function, β, is a beam optics quantity, which is determined by the accelerator magnet configuration. ϵ and β are related by

$$\epsilon = \pi\sigma^2/\beta. \tag{2.9}$$

To achieve a high luminosity for the beam, Eq. (2.8) implies that we need β^* to be as small as possible; and that depends on the capability of the hardware to make a near-focus at the interaction point. In addition, Eq. (2.8) also implies that, to achieve the high luminosity, we need to have large number of bunches with low emittance collide at high frequency at location where the beam optics gives as low values of the amplitude functions as possible.

Luminosity is often expressed in $cm^{-2}s^{-1}$ and usually comes in high order of magnitude. For example, at KEK, its B-factory for electron-positron collider had recently reached a peak luminosity in excess of 10^{34} $cm^{-2}s^{-1}$. The highest luminosity for the protons collider achieved so far is 1.3×10^{32} $cm^{-2}s^{-1}$.

2.6 Luminosity Measurement Methods

There are three general methods to measure luminosity for a colliding accelerator: 1) luminosity measurement method using beam parameters for the case that the beam parameters can be obtained with good accuracy, 2) The optical theorem method and 3) luminosity measurement method using known cross-section and event rate. There have been ongoing investigations on all these three methods, but none has promised practical result on reaching the required precision level of the LHC.

In this section, we discuss some difficulties involving each method and then focus on discussing the method we use in this thesis, the $W^{\pm}$ and Z^0 production method.

2.6.1 Luminosity measurement using beam parameters

In this method, a sound measurement of the lateral beam size as well as of the bunch currents are needed. To obtain reliable Gaussian transverse beam values, ρ, from the beam sizes, the β-function has to be known precisely, which typically could yield uncertainty up to 10%. One way to measure the beam width at the interaction point, which is potentially accurate, is the "van der Meer" method based on transverse beam scans. Originally [13], this was done by moving one beam vertically and at the same time recording the relative change of the rate of proton-proton interactions. In the case of the LHC, such scans are very difficult for low-β^* running since the beam-beam interactions are very strong and may affect the beam sizes while the scans are performed. Additionally, the beam size would be small (16 μm), and thus dedicated run with large values of β^* (at least 50 m) are required. Another complication is due to the non-zero crossing angle which causes a longitudinal shift of the interaction point (and hence a change of the beam size), while one beam is moved transversely.

To summarize, the van der Meer method demands dedicated runs at high-β^* and very low luminosity ($< 10^{30}$ cm^{-2}s^{-1}), and to reach an accuracy of better than 5-10% on the luminosity measurement, the goal of the LHC, is unlikely to be feasible. Moreover, a regular beam scans at high luminosity are considered impractical.

2.6.2 Luminosity measurement using optical theorem

This method makes use of the optical theorem in high-energy scattering from the relation

$$\mathcal{L}\frac{dR_{el}}{dt}|_{t=0} = R_{tot}^2(1+\rho^2)/(16\pi), \tag{2.10}$$

where R_{tot} is the total rate of proton-proton interactions, $dR_{el}/dt(t = 0)$ is the rate of forward elastic scattering, ρ is the ratio of the real and imaginary part of the elastic forward amplitude. The major challenge of this method is the ability to detect the very forward elastically-scattered protons. We need to make a simultaneous measurements of the total interaction rate and the rate of forward elastic scattering. The total interaction rate has to be measured using detectors at large angles to the beams and covering a wide range in rapidity, y (see Appendix A).

From preliminary investigation, the large angle and rapidity acceptance could be achieved by installing addition of dedicated detector parts. In addition, measuring ρ, the ratio of the real to imaginary part of the elastic forward amplitude Eq. (2.10) at the LHC is considered very difficult according to W. Kienzle et al [14]).

To summarize, to be able to obtain accurate result of such detection in optical theorem method, we need additional installation of the detectors and particular running conditions at a luminosity less than about 10^{32} cm^{-2}s^{-1} to be free from pile-up effect. To reach an accuracy better than 5-10% for luminosity measurement using optical theorem is considered very difficult unless a very high and well understood efficiency for inelastic events can be done.

2.6.3 Luminosity measurement using production of particular processes

For the case that a process's cross-section can be accurately measured, Eq. (5.3) is applied to obtain the luminosity. In previous experiments at LEP, high precision of luminosity was obtained with the use of $e^+e^- \to e^+e^-$ process at small momentum transfer. This process was well predicted by the successful QED physics, and thus could give accurate cross-section to determine the luminosity to within 1% error. Under a similar scheme, there are proposals to measure the luminosity of the LHC using particular processes [15], [16] and [17]. Two processes are in particular attentions; lepton pair production and the $W^{\pm}$ and Z^0 production. According to [1], the two processes are expected to resolve the difficulty of achieving precision of 5% for the luminosity measurement program at the LHC.

In this thesis, we have focused our study on the possibility of using the $W^{\pm}$ and Z^0 production to measure the luminosity at the LHC. In the section below, we give some brief discussion for the $W^{\pm}$ and Z^0 production method.

$W^{\pm}$ and Z^0 Production Method

The $W^{\pm}$ and Z^0 production is a promising process to measure the luminosity because the three particles, W^+, W^- and Z^0 will be produced at high rates at the LHC (see Fig. 2.2). Moreover, their signatures through leptonic decay modes, $W^{\pm} \rightarrow l^{\pm}\nu(\bar{\nu})$, $Z \rightarrow l^+l^-$ are clean and well measurable in high energy proton-proton collision [17], [15].

Another important key ingredient is that the cross-sections of the $W^{\pm}$ and Z^0 production at the LHC can be theoretically calculated to high accuracy. Recent determinations of $W^{\pm}$ and Z^0 cross-sections can be found in References [18] and [19]. In these two references, the theoretical calculation up to the next-to-next-to-leading order (NNLO) has been made; some of the calculated results are displayed in Fig. 2.3. Except from the last two dots on the right-handed side, Fig. 2.3 shows that $\pm$ 5%, is the upper limit on the uncertainty on σ_W and σ_Z at LHC.

In the results on the work performed by V.A. Khoze et al., in 2000 [17], they have concluded that, **allowing all uncertainties, the cross-sections of $W^{\pm}$ and Z^0 production are known to be about $\pm$4% at the LHC energy**. Some theorists predict that these uncertainties will be as low as $\pm(1-2)$% by the time the LHC is turned on. However, the results are only theoretical predictions. In the real situation when the LHC starts operating and the data is collected from the detector, the uncertainty of this method will also depend on the the smearing of particles in the detector, the pile-up effect from electronic readout response and possible background from other physics processes. We do not yet know how do these effects will act upon the uncertainty of the luminosity measurement. It is in this work that they are investigated.

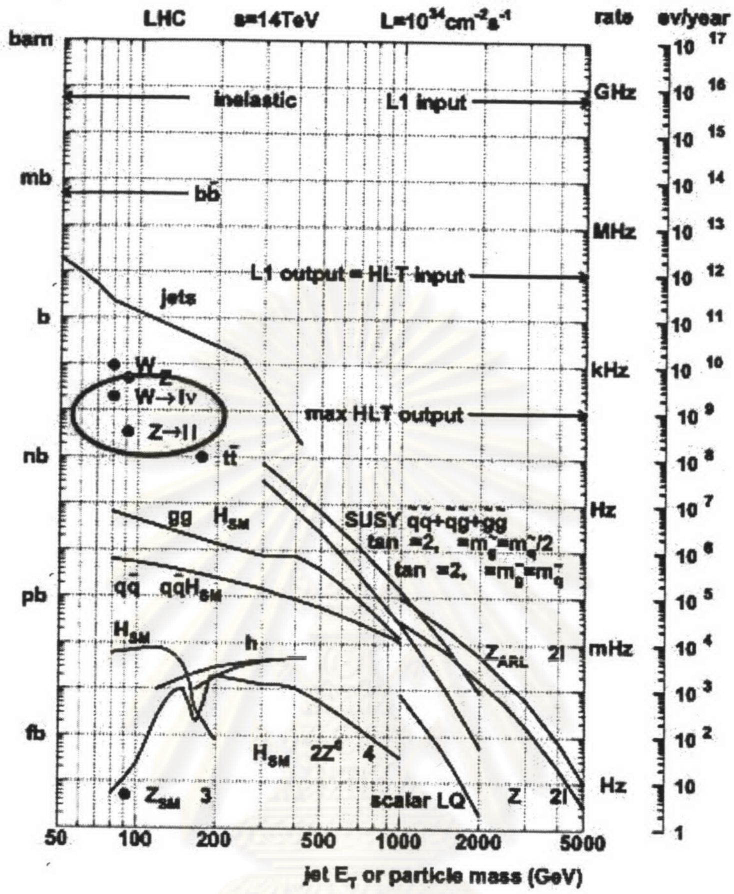

Figure 2.2: The event rates of particles production at the LHC at "nominal luminosity." (picture from CERN Internal Note, 1983)

2.7 Physics of Weak Boson Production at the LHC

In the proton-proton collision, the weak bosons are produced from weak interaction among quarks and leptons. The dominant Feynman diagrams for the weak bosons production at the LHC are shown in Fig. 2.4 and Fig. 2.5. The anti-quark in the proton-proton collision comes from the sea quark, while the quark could come from either a valence quark or a sea quark. Below, we discuss the two channels of $W^{\pm}$ and Z^0 production those we have investigated in this thesis.

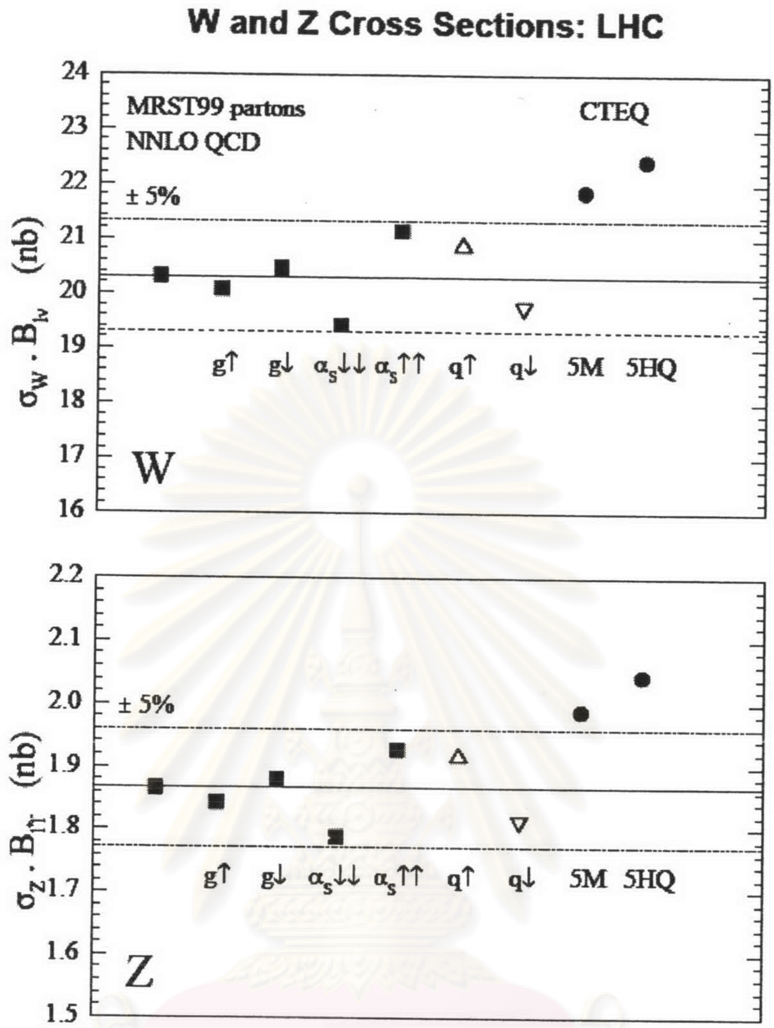

Figure 2.3: The theoretically calculated cross-sections for W and Z production times leptonic branching ratios in pp collisions at 14 TeV using the MRST99, CTEQ5M and CTEQ5HQ parton sets (picture from A.D. Martin, R.G. Roberts, W.J. Stirling and R.S. Thorne. *Eur. Phys. J. C* **14** (2000) 133).

2.7.1 The $W^{\pm}$ Production: $q\bar{q} \rightarrow W^{+}W^{-} \rightarrow l^{\pm}\nu_l(\bar{\nu}_l)$

The type of $W^{\pm}$ production and decay process at the LHC that will only be studied in this thesis is: $q\bar{q} \rightarrow W^{+}W^{-} \rightarrow l^{\pm}\nu_l(\bar{\nu}_l)$. The "invisible" neutrino part of the process makes the reconstruction of the $W^{\pm}$ more complicated than the case of Z^0. The decay product of the W^+ and W^- are, respectively, only $l_R^+\nu_L$ and only $l_L^-\bar{\nu}_R$, where the ν_L have positive helicity and the $\bar{\nu}_R$ have negative helicity. Helicity is a

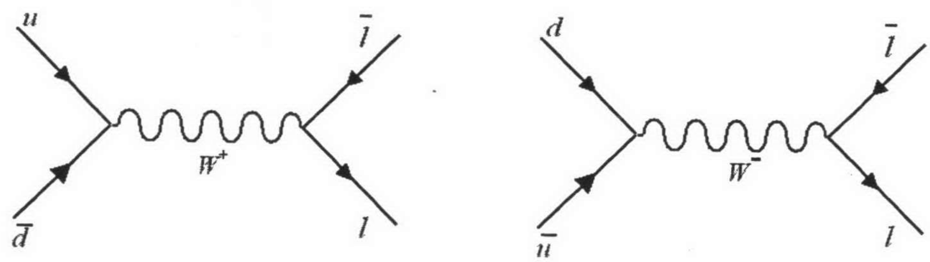

Figure 2.4: Feynman Diagram of $W^{\pm}$ Production at LHC.

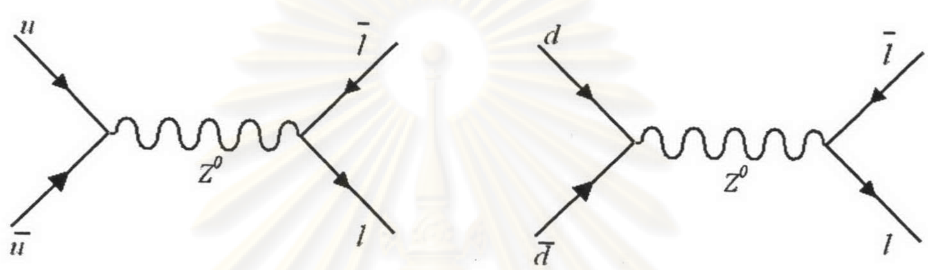

Figure 2.5: Feynman Diagram of Z^0 Production at LHC.

quantum number of value m_s/s. A particle of spin $\frac{1}{2}$ can have a helicity of +1 ($m_s = \frac{1}{2}$) and -1 ($m_s = -\frac{1}{2}$); they are called "right-handed (R)" and "left-handed (L)" particle respectively. It has been known from extensive experimental observation that there are only left-handed neutrinos (ν_L) and right-handed antineutrinos ($\bar{\nu_R}$) in nature. In weak interaction, the V-A (vector minus axial vector) theory [20] must hold; therefore we only have $l_R^+\nu_L$ and only $l_L^-\bar{\nu}_R$ as decay product of $W^{\pm}$.

2.7.2 The Z^0 Production: $q\bar{q} \rightarrow Z^0Z^0 \rightarrow 2l^+2l^-$

The process is originated from $u\bar{u}$ and $d\bar{d}$ annihilations which has a clean signal through $Z^0 \rightarrow l^+l^-$ process. If the two leptons are muons, they can be well measured at the CMS detector and thus could provide well reconstruction of the Z^0 four momentum. The event rate of this process is expected to be about a factor of 5 - 10 times smaller than those of the $W^{\pm}$ at the LHC. But, this number is still considered very high.

The differential cross-section for this process [21] can be calculated from

$$\frac{d\sigma}{d\hat{t}}(q_i\bar{q}_i \to Z^0Z^0) = \frac{\pi\alpha^2(L_i^4+R_i^4)}{96x_W^2(1-x_W)^2\hat{s}^2}\left[\frac{\hat{t}}{\hat{u}}+\frac{\hat{u}}{\hat{t}}+\frac{4M_Z^2\hat{s}}{\hat{t}\hat{u}}M_Z^4\left[\frac{1}{\hat{t}^2}+\frac{1}{\hat{u}^2}\right]\right], \quad (2.11)$$

where the average over the initial quark colors and statistical factor of $\frac{1}{2}$ for identical particles in the final states are taken.